Effect of organic micropollutants on biofouling in a forward osmosis process integrating seawater desalination and wastewater reclamation

Kim, Youngjin; Kim, Lan Hee; Vrouwenvelder, Johannes S.; Ghaffour, Noreddine

DOI
10.1016/j.jhazmat.2020.123386

Publication date
2021

Document Version
Final published version

Published in
Journal of Hazardous Materials

Journal of Hazardous Materials 401 (2021) 123386

Contents lists available at ScienceDirect

Journal of Hazardous Materials

journal homepage: www.elsevier.com/locate/jhazmat

Effect of organic micropollutants on biofouling in a forward osmosis process integrating seawater desalination and wastewater reclamation

Youngjin Kim[a], Lan Hee Kim[b], Johannes S. Vrouwenvelder[b,c], Noreddine Ghaffour[b,*]

[a] Department of Environmental Engineering, Sejong Campus, Korea University, 2511, Sejong-ro, Jochiwon-eup, Sejong-si, 30019, Republic of Korea
[b] King Abdullah University of Science and Technology (KAUST), Water Desalination and Reuse Center (WDRC), Division of Biological & Environmental Science & Engineering (BESE), Thuwal 23955-6900, Saudi Arabia
[c] Department of Biotechnology, Faculty of Applied Sciences, Delft University of Technology, Van der Maasweg 9, 2629 HZ Delft, the Netherlands

GRAPHICAL ABSTRACT

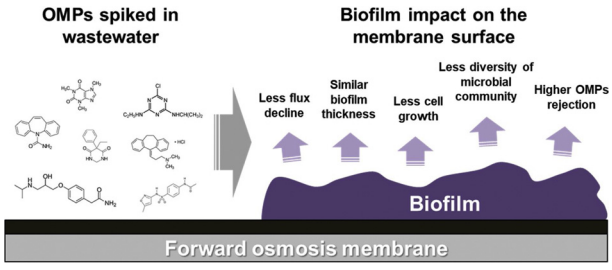

ARTICLE INFO

Editor:D. Aga

Keywords:
Forward osmosis (FO)
Organic micropollutants (OMPs)
Biofouling
Osmotic dilution
Next-generation sequencing
Optical coherence tomography (OCT)

ABSTRACT

This study systematically investigated the effect of organic micropollutants (OMPs) on biofouling in forward osmosis (FO) integrating wastewater treatment and seawater dilution. Synthetic seawater (0.6 M sodium chloride) was used as a draw solution and synthetic municipal wastewater as a feed solution. To evaluate the impact of OMPs in a replicate parallel study, wastewater was supplemented with a mixture of 7 OMPs (OMPs-feed) and without OMPs (control) during 8 batch filtration cycles with feed and draw solution replacement after each filtration. The FO performance (water flux), development and microbial composition properties of biofilm layers on the wastewater side of the FO membrane were studied. Compared to the control without OMPs, the FO fed with OMPs containing wastewater showed (i) initially the same water flux and flux decline during the first filtration cycle, (ii) with increasing filtration cycle a lower flux decline and (iii) lower concentrations for the total cells, ATP, EPS carbohydrates and proteins in biofilm layers, and (iv) a lower diversity of the biofilm microbial community composition (indicating selective pressure) and (v) increasing rejection of 6 of the 7 OMPs. In essence, biofouling on the FO membrane showed (i) a lower flux decline in the presence of OMPs in the feed water and (ii) a higher OMPs rejection, both illustrating better membrane performance. This study has a significant implication for optimizing osmotic dilution in terms of FO operation and OMPs rejection.

1. Introduction

To overcome water scarcity of fresh water, seawater desalination is getting increasing attraction as an alternative water source due to the abundant amount if seawater/ocean (Badran, 2017) and the fact that a large number of the world's population lives within 100 km from the coastline (Liu et al., 2015; Barragán and de Andrés, 2015). Seawater reverse osmosis (SWRO) desalination process has been getting

* Corresponding author.
E-mail address: noreddine.ghaffour@kaust.edu.sa (N. Ghaffour).

https://doi.org/10.1016/j.jhazmat.2020.123386
Received 24 February 2020; Received in revised form 2 June 2020; Accepted 2 July 2020
Available online 04 July 2020

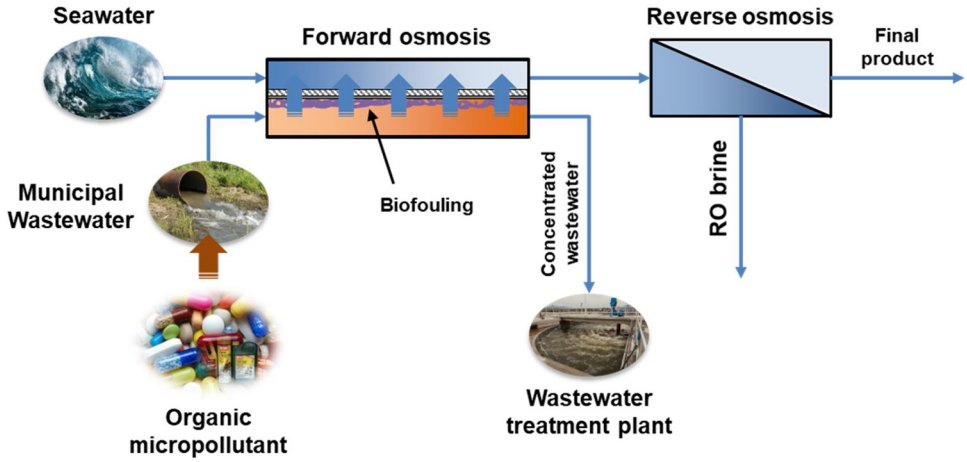

Fig. 1. Schematic diagram of a forward osmosis (FO) and reverse osmosis (RO) hybrid process integrating seawater desalination and wastewater reclamation. Municipal wastewater containing organic micropollutants (OMPs) and seawater are fed into the FO process as FS and DS, respectively. The diluted seawater can be treated by a lower energy (lower cost) RO process to produce fresh water.

increasing attention owing to its lower energy consumption (3 ~ 4 kW h m^{-3}) compared to other mature processes, namely multi-stage flash (MSF, 10 ~ 16 kW h m^{-3}) and multiple-effect distillation (MED, 5.5 ~ 9 kW h m^{-3}) (Ghaffour et al., 2013). Compared to the conventional water treatment technologies (e.g., 0.38 kW h m^{-3} for Qingdao, China) (Smith and Liu, 2017), the energy consumption of SWRO is still very high, which hampers the drinking water application.

A forward osmosis (FO, also called osmotic dilution) and reverse osmosis (RO) hybrid process (Fig. 1), which integrates seawater desalination and wastewater reclamation, was proposed as a novel energy-efficient hybrid desalting process (Cath et al., 2010). In FO, seawater used as draw solution (DS) is diluted and then supplied to RO. Simultaneously, wastewater with low salinity, such as municipal wastewater, is utilized as a feed solution (FS) to create a driving force. Therefore, the FO-RO hybrid process can not only achieve 25 % specific energy-saving (Attarde et al., 2017; Wei et al., 2019) but also reduce the environmental impact by more than 25 % (Hancock et al., 2012) compared to RO alone. Life-cycle cost analysis also showed that the hybrid process can have a 56 % lower operating expenditure (OPEX) but 21 % higher capital expenditure (CAPEX) than SWRO alone (Valladares Linares et al., 2016a). The FO-RO hybrid process also has a benefit in terms of high rejection owing to its multiple-barrier effect. Rejection rate of ion and organic content by pilot-scale FO-RO hybrid system was above 96 % nitrate and more than 99.9 % removal of dissolved organic carbon (DOC) (Hancock et al., 2013). In addition, the FO-RO hybrid system exhibited a stable water flux and high rejection of dissolved organic matters (Xie and Gray, 2016).

To optimize the FO-RO hybrid system, several studies have been conducted (Bamaga et al., 2011; Blandin et al., 2015; Kim et al., 2018; Kook et al., 2018). They suggested that membrane performance should have at least a water flux of 30 L m^{-2} h^{-1}, water permeability of higher than 5 L m^{-2} h^{-1} bar^{-1}, and the structural parameter of lower than 100 μm for economical operation (Blandin et al., 2015). Despite these efforts, the efficient operation of the FO-RO hybrid process can be hampered by membrane fouling, mainly caused by the utilization of wastewater as FS. In FO integrating seawater and municipal wastewater, seawater as DS did not have any influence on membrane fouling because of the direction of water flux, while wastewater as FS caused severe water flux decline due to organic foulants (Boo et al., 2013). When treating real secondary effluent, significant flux decline was observed, but the water flux was very effectively recovered by hydraulic flushing (Choi et al., 2016; Kim et al., 2020). It was also found that primary effluent induced a more severe flux decline than secondary effluent (Volpin et al., 2018). A pilot-scale FO-RO hybrid study demonstrated that FO membrane has high reversibility, and FO can reduce membrane fouling in RO (Choi et al., 2017).

Since municipal wastewater is utilized as FS, the presence of organic micropollutants (OMPs) may be able to lead to some potential problems (e.g., poor quality of product water) in the hybrid system (Giwa et al., 2019). Since FO utilizes DS with high concentration, reverse diffusion of draw solutes to the FS hinders the forward transport of the OMPs, thereby achieving higher rejection than RO (Xie et al., 2012a; Volpin et al., 2019). In addition, rejection of OMPs by FO membranes can be influenced by many factors such as membrane type (e.g., polyamide, cellulose triacetate), membrane orientation, feed solution pH and temperature, membrane fouling, and membrane surface properties. Thin-film composite (TFC) polyamide (PA) membrane showed high rejection of the OMPs than cellulose triacetate (CTA) membrane due to the pore hydration of the TFC PA membrane (Xie et al., 2014a; Akther et al., 2019; Jin et al., 2012). Membrane orientation also has a significant impact on the OMPs rejection because of a highly porous support layer (Xie et al., 2012b). Operation parameters such as water flux, solution pH and temperature play a dominant role to determine OMPs rejection. High water flux resulted in high rejection of OMPs due to the dilution effect (Xie et al., 2014b; Kim et al., 2017a). Solution pH remarkably affected the rejection of ionic OMPs because pH changed surface charges of FO membrane and the OMPs (Xie et al., 2012b). Solution temperature changed solution properties as well as FO performance (Lee and Ghaffour, 2019) and hence influenced OMPs rejection (Xie et al., 2013). Membrane fouling and its surface characteristics also have a significant impact on OMPs rejection (Xie et al., 2014b; Kim et al., 2017a; Valladares Linares et al., 2011). In the meantime, OMPs have a significant potential to influence membrane fouling, particularly biofouling, because OMPs may be able to either accelerate or decelerate the growth of microorganisms (Żur et al., 2018). Until now, nevertheless, the potential impact of the OMPs on biofouling in FO has not been investigated.

Therefore, this study aims to investigate the effect of the OMPs on biofouling in FO (i.e., an osmotic dilution process integrating seawater desalination and wastewater reclamation). For this, FO performance in terms of flux decline was first investigated with and without seven different OMPs (amitriptyline hydrochloride, atenolol, atrazine, caffeine, carbamazepine, primidone, sulfamethoxazole) in the FS. Biofilm growth was simultaneously evaluated using an optical coherence tomography (OCT) during FO operation cycles (8 cycles). After experiments, biofilm was extracted and analyzed to investigate the effect of the OMPs on the property of the biofilm. To evaluate the effect of the OMPs on the bacterial community composition of the biofilm, next-generation sequencing (NGS) was carried out. Lastly, the effect of the biofilm on OMPs removal was evaluated when treating synthetic municipal wastewater. In this study, we report the first comprehensive investigation on the effect of OMPs on biofouling in FO with a significant implication for optimizing osmotic dilution in terms of FO operation and OMPs rejection.

Table 1
Analysis of primary wastewater sampled from King Abdullah University of Science and Technology (KAUST, Saudi Arabia) wastewater treatment plant.

Parameters	Values
pH	7.32 ± 0.19
Conductivity	529 ± 124 μS cm^{-1}
Dissolved organic carbon (DOC)	147.6 ± 14.8 mg L^{-1}
Chemical oxygen demand (COD)	178 ± 3.5 mg L^{-1}
Total nitrogen (TN)	205.2 ± 6.5 mg L^{-1}
Total cells	9.04 ± 1.58 × 10^9 cells L^{-1}

2. Materials and methods

2.1. FO membrane

Thin-film composite (TFC) polyamide (PA) FO membrane was purchased from Toray Korea and then stored in deionized (DI) water at 4 °C until use. Detailed information on the FO membrane used in this study can be found elsewhere (Kim et al., 2017b).

2.2. Feed and draw solutions

Primary wastewater was sampled from a wastewater treatment plant located in King Abdullah University of Science and Technology (KAUST, Saudi Arabia) to inoculate the FO wastewater with bacteria for initial biofilm development on the active layer of FO membrane (i.e., the wastewater side). Detailed information of primary wastewater is presented in Table 1. Synthetic municipal wastewater was used as a FS, and its composition can be found elsewhere (Kim et al., 2017a). 0.6 M sodium chloride (NaCl) was utilized as a DS to simulate seawater. All chemicals were received at reagent grade from Sigma Aldrich (USA).

Seven different OMPs (i.e., amitriptyline hydrochloride, atenolol, atrazine, caffeine, carbamazepine, primidone, and sulfamethoxazole) were selected as the representatives of pharmaceutically active compounds, personal care products, household chemicals, and pesticides because they are often observed in municipal wastewater and have a low removal propensity in the biological process (Wei et al., 2015). These OMPs were purchased from Sigma Aldrich (USA). Their key physicochemical characteristics are presented in Table 2. To prepare a stock solution of 17.5 g·L^{-1} OMPs (i.e., 2.5 g·L^{-1} concentration for each OMPs), 2.5 mg of each OMPs were added to 1 mL of HPLC grade methanol. For an analysis of OMPs concentrations in FS and DS, the stock solution of isotopes corresponding to the OMPs was also prepared by dissolving 0.25 mg of each isotope in 100 mL HPLC grade methanol. Stock solutions were stored at 4 °C. All procedures for the preparation of OMPs stock solution and isotope stock solution are summarized in **Fig. S1**.

2.3. Lab-scale FO biofouling experiments

A lab-scale FO system, consisting of a custom-made FO flow cell with two channels (i.e., 100 mm length, 20 mm width and 3 mm depth), two gear pumps, two reservoirs (each with a 2 L volume), two flow meters, a balance, and a magnetic stirrer, was employed in this study. The magnetic stirrer was utilized for the continuous mixing of the FS. The DS reservoir was placed on a balance (Mettler Toledo, USA) to monitor the changes in the DS weight.

FO experiments were conducted for 8 days under the active layer facing feed solution (AL-FS) mode to evaluate biofouling in FO. Real primary wastewater was firstly circulated in the FS channel for 24 h without DS circulation to ensure the biofilm formation by its high cell concentration (9.04 ± 1.58 × 10^9 cells L^{-1}). Subsequently, only synthetic municipal wastewater was used as a FS, and 0.6 M NaCl was employed as a DS to represent seawater. The crossflow velocities for the feed and draw side were 8.5 cm s^{-1} under a counter-current direction. Solution temperature was maintained at room temperature (25 ± 1 °C). Both FS and DS were freshly replaced every day. The detailed descriptions of FO biofouling experiments are available elsewhere (Bucs et al., 2016) and presented briefly in **Fig. S2**. In order to investigate the effect of the OMPs on biofouling, 20 μL of OMPs stock solution was spiked into 2 L of feed solution every day to obtain a final concentration of 25 μg L^{-1}. In addition, 20 μL of methanol was injected into another 2 L feed solution every day for comparison with the effect of the OMPs because methanol can influence the biofilm growth as an additional carbon source. Water flux was measured in time using a balance connected to a computer, and normalized water flux was calculated by dividing water flux by initial water flux at 1st run.

2.4. Biofilm characterization

Biofilm growth on the FO membranes was monitored at operation days of 1, 4, and 8 (i.e., 1st run, 4th run and 8th run, respectively) using an OCT (Thorlabs GANYMEDE SD-OCT, Thorlabs, Germany) equipped with a 5 × telocentric scan lens (LSM03-BB, Thorlabs, Germany). Biofilm growth was observed at the feed side-membrane layer, while a biofilm on the draw-side of the membrane layer was not observed. This absence of biofilm is most likely caused due to the high rejection of the FO membrane, the relative high purity of the DS (synthetic seawater), and the direction of water flux (Kim et al., 2015a). The averaged biofilm thickness was obtained from 50 different locations of the fouled membrane. In this study, an OCT equipment was employed to analyze the biofilm structure because of its substantial benefit of allowing real-time monitoring of the biofilm structure non-destructively during FO experiments. OCT has been demonstrated and widely accepted as a suitable tool for biofilm studies (Fortunato et al., 2018; Dreszer et al., 2014; Valladares Linares et al., 2016b).

To characterize biofilm layers on the FO membranes, membrane coupons were collected after biofouling experiments and then cut into 6 pieces for biofilm analysis. In this study, the biofouling was observed only on the active layer (i.e., wastewater side), and thus the analysis results represented the biofilm on the active layer. For DOC analysis, the membrane coupon (20 mm × 10 mm) was soaked in 10 mL of MilliQ (MQ) water, and biofilm was extracted using vortexing followed by sonication. The solution was filtered by 0.45 μm pore size syringe

Table 2
Physicochemical properties of seven organic micropollutants (OMPs) used in the present study. Data was adopted from Wei et al. (Wei et al. (2015)).

Compounds	Application	Formula	Molecular weight (g mol^{-1})	Charge	Log D[a]
Amitriptyline hydrochloride	Antidepressant	$C_{20}H_{24}ClN$	313.87	+	2.28
Atenolol	Beta-blocker	$C_{14}H_{22}N_2O_3$	266.34	+	−2.09
Atrazine	Herbicide	$C_8H_{14}ClN_5$	215.69	N[b]	2.64
Caffeine	Stimulant	$C_8H_{10}N_4O_2$	194.19	N	−0.63
Carbamazepine	Anticonvulsant	$C_{15}H_{12}N_2O$	236	N	1.89
Primidone	Anticonvulsant	$C_{12}H_{14}N_2O_2$	218.25	N	0.83
Sulfamethoxazole	Antibiotic	$C_{10}H_{11}N_3O_3S$	253.28	–	−0.22

[a] Log D: the distribution coefficient (high Log D indicates high hydrophobicity); [b] N: neutral charge.

filter, and DOC was then measured via a TOC analyzer (TOC-V_{CPH}, Shimadzu, Japan). For adenosine triphosphate (ATP) analysis, the biofilm on the membrane coupon (20 mm × 10 mm) was extracted in 10 mL dechlorinated tap water. Then ATP was measured using the ATP analyzer (Advance™, Celsis, USA). To quantify cell numbers in biofilm layers, the biofilm on the membrane coupon (20 mm × 10 mm) was dissolved in 10 mL of 1 × phosphate-buffered saline (PBS) solution, and the cell numbers were measured using a BD Accuri™ C6 flow cytometry (BD Biosciences, USA).

For the extracellular polymeric substances (EPS) measurement, the biofilm on the membrane coupon (20 mm × 30 mm) was dissolved in 10 mL PBS solution using 2 min of vortexing and 5 min of sonication. A detailed procedure of EPS characterization can be found elsewhere (Kim et al., 2015b). The solution was treated at 4 °C with 60 µL of formaldehyde (37 %) for 1 h followed by 4 mL of 1 N NaOH solution for 3 h. Afterward, the solution was centrifuged at 20,000 × *g* for 20 min. Then, the supernatant was filtered by a 0.2 µm pore-sized syringe filter and dialyzed using a 3.5 K MWCO dialysis membrane for 24 h. The solution was freeze-dried using a freeze-dryer (Martin Christ, Germany). Lastly, the samples were adjusted to 10 mL by adding MQ water. The concentration of the carbohydrate and protein-EPS in the samples were measured by a SpectraMax 340PC microplate reader (Molecular Devices, USA). Fluorescence excitation-emission matrix (FEEM) of the samples was analyzed using a fluorescence spectrometer (FluoroMax, HORIBA, Japan) under excitation of 220 nm–400 nm and emission of 270 nm–500 nm.

Another membrane coupon (20 mm × 20 mm) was dried in a desiccator for 24 h for further analyses. Fouled FO membranes were coated with iridium and analyzed by scanning electron microscopy (SEM, Zeiss Merlin, Carl Zeiss AG, Germany) and energy dispersive X-ray spectroscopy (EDX) at an accelerating voltage of 3 kV and 20 kV, respectively. Averaged roughness of fouled FO membrane surface was measured using atomic force microscopy (AFM, Dimension Icon, Bruker, Germany) under ambient conditions in non-contact mode with silicon probes. Fourier transform infrared (FT-IR) spectra of fouled FO membranes were obtained under wavelength ranging from 500 cm^{-1} to 4000 cm^{-1} using a FT-IR spectrometer (Spectrum 100, PerkinElmer, USA).

2.5. Next-generation sequencing (NGS) analysis

Genomic DNA extraction from the fouled membranes was performed using a DNeasy PowerWater kit (Qiagen, Germany). Bacterial 16S rRNA gene (V1-V3 region) sequencing libraries were prepared (Caporaso et al., 2012). 10 ng of extracted DNA was amplified by polymerase chain reaction (PCR), and the amplicon libraries were purified using Agencourt Ampure XP beads (Beckman Coulter, USA). For DNA sequencing, the purified sequencing libraries were pooled in equimolar concentrations and diluted to 6 nM. The samples were paired-end sequenced (2 × 300 bp) on a MiSeq (Illumina, USA) using a MiSeq Reagent kit v3 (Illumina, USA). For bioinformatic processing, forward and reverse reads were trimmed and merged using FLASH v. 1.2.7 (Magoč and Salzberg, 2011). OTU (operational taxonomic unit) abundances were estimated using the UPARSE workflow (Edgar, 2013), and taxonomy was obtained using the RDP classifier (Wang et al., 2007). The results were analyzed in R 3.5.0 via the R studio IDE using the ampvis package v.2.4.0 (Albertsen et al., 2015). A detailed procedure of bacterial community composition analysis via pyrosequencing can be found elsewhere (Kim et al., 2017a).

2.6. Organic micropollutants (OMPs) analysis

After the experiments at 1st run and 8th run, 100 mL of samples were collected and spiked with 10 µL of isotopes (Cambridge Isotope Laboratories, Inc., USA). Solid-phase extraction (Dione Autotrace 280 and Oasis cartridges) was then conducted to extract the OMPs from the samples. OMPs extraction was concentrated up to 1 mL via evaporation at a temperature of 60 °C for 1 h. Finally, the concentration of OMPs were measured using liquid chromatography (Agilent Technology 1260 Infinity LC unit, USA) followed by mass spectrometry (AB SCIEX QTRAP 5500 mass spectrometer, Applied Biosystems, USA). A detailed procedures of OMPs analysis can be found elsewhere (Kim et al., 2019a). OMPs rejection can be obtained by Eq. (1).

$$R_{OMPs} = \left(1 - \frac{C_{OMPs} \times V_D/V_P}{C_{OMPs,f}}\right) \times 100\% \quad (1)$$

where R_{OMPs} is the rejection rate (%) of OMPs, C_{OMPs} and $C_{OMPs,f}$ are the concentration of OMPs (µg·L^{-1}) in the DS and FS, respectively, and V_D and V_P are the respective volumes (L) of the DS and the permeate after FO experiments.

3. Results and discussion

3.1. Influence of organic micropollutants (OMPs) on FO performance

In this study, FO experiments were conducted with or without 25 µg·L^{-1} each OMPs (total 175 µg·L^{-1}) in FS to investigate the effect of the OMPs on the FO performance during wastewater treatment and seawater dilution. “OMPs-feed” and “control” will refer to FO experiments with OMPs and without OMPs (only methanol), respectively, unless stated otherwise. The experimental results show that similar initial water flux between OMPs-feed and control of 20.7 ± 1.2 L m^{-2} h^{-1} and 22.4 ± 0.4 L m^{-2} h^{-1}, respectively. The results implies that the presence of the OMPs does not significantly influence water flux in FO due to much lower concentration (175 µg·L^{-1}) of OMPs compared to that (550 mg L^{-1}) of synthetic municipal wastewater.

For the comparison of flux decline between control and OMPs-feed, the resulting water fluxes were normalized and presented in Fig. 2. Similar flux decline (i.e., 22.8 ± 2.6 % and 21.4 ± 1.8 %, respectively) from initial water flux of 22.4 ± 0.4 L m^{-2} h^{-1} and 20.7 ± 1.2 L m^{-2} h^{-1} for control and OMPs-feed was observed for both experiments during the 1st run. Afterward, both FS and DS were refreshed in order to restore the driving force (the effective osmotic pressure gradient), which was decreased by the concentration of the FS

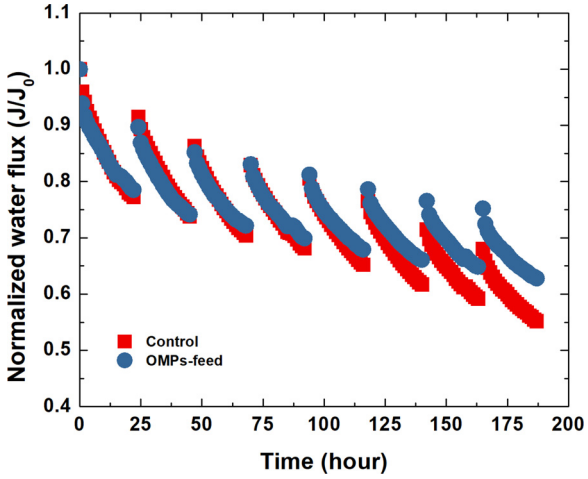

Fig. 2. Normalized flux decline curves for 8 days (8 cycles) FO operation. Control represents FO experiments without OMPs, and OMPs-feed represents FO experiments with OMPs spiking. Experimental conditions of FO experiments: synthetic municipal wastewater as FS, 0.6 M NaCl as DS, crossflow velocity of 8.5 cm·s^{-1}, and temperature of 25 ± 0.5 °C. Prior to FO experiments, the membrane was conditioned for 24 h using primary wastewater. FS and DS were replaced with fresh solutions everyday. FO experiments were performed in duplicate, and the average values are shown in Fig. 2.

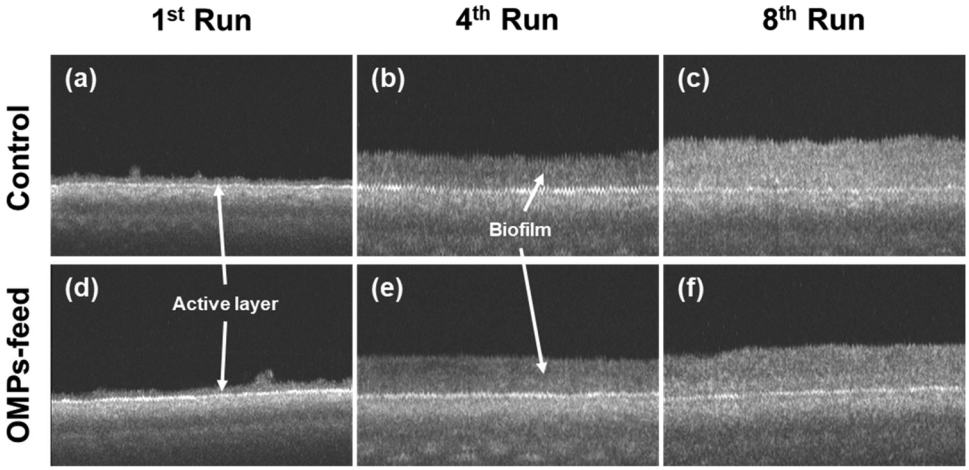

Fig. 3. OCT images of control at (a) 1st run, (b) 4th run, and (c) 8th run of FO operation, and OMPs-feed at (d) 1st run, (e) 4th run and (f) 8th run of FO operation. The black area indicates the channel filled with the FS. The dark gray area and the white line indicate the support layer and the active layer of the FO membrane. The thin gray area between the channel and the active layer indicates the fouling layer (i.e., the biofilm).

and the dilution of the DS. Then, decreased initial water fluxes of the 2nd run were observed compared to those of the 1st run, which indicates that membrane fouling occurred. Until the 5th run, initial water fluxes of both control (80.6 ± 5.2 %) and OMPs-feed (81.3 ± 0.9 %) were similar at 1st run, but interestingly, control showed severer flux decline (i.e., 34.8 ± 2.9 % and 32.1 ± 1.5 %) than OMPs-feed when compared to initial water flux at 1st run. From the 6th run, control started to exhibit lower initial water flux as well as higher flux decline than OMPs-feed, thereby resulting in a flux decline of 44.8 ± 4.4 % and 37.1 ± 2.7 % for control and OMPs-feed after the 8th run. The results indicate that OMPs might mitigate the formation of membrane fouling on the membrane surface because the FS and DS were replaced every day.

3.2. Influence of organic micropollutants (OMPs) on biofouling in FO

To monitor the development of the fouling layer in real time, an OCT analysis was conducted on the membrane surface of control and OMPs-feed during the 1st run, 4th run and 8th run, as presented in Fig. 3. In OCT images, the black area indicates the channel filled with the FS. The dark gray area and the white line indicate the support layer and the active layer of the FO membrane, respectively. Therefore, the thin gray area between the channel and the active layer indicates the fouling layer (i.e., the biofilm). To accelerate the biofilm growth, the membrane surface was conditioned/inoculated with primary wastewater containing microorganisms for 24 h before the wastewater treatment. During the 1st run, therefore, the thin fouling layer was observed on the active layer, as shown in Figs. 3a and d. To analyze the fouling layer quantitatively, we also measured thicknesses at 50 different locations of the biofilm and reported the average values in Table 3. The thickness of the fouling layer was 32.1 ± 18.8 μm and 25.2 ± 10.2 μm for control and OMPs-feed, respectively at the 1st run. After 3 days of operation (4th run), the fouling layer became thicker, as shown in Fig. 3b and e. Nevertheless, their thicknesses were still similar, 89.0 ± 12.9 μm and 87.7 ± 21.9 μm. On the last day (8th run) of FO operation, the biofilm became thicker than the previous biofilm, and control (Fig. 3c) exhibited a little bit thicker biofilm than OMPs-feed (Fig. 3f). However, the difference in measured thicknesses was not significant (i.e., 125.4 ± 41.4 μm and 117.7 ± 29.4 μm). The similar biofilm thickness between OMPs-feed and control indicates that OMPs does not impact on biofilm structure (or morphology).

Table 3
The average thickness of the biofilm at 1st run, 4th run, and 8th run of FO operation. Averaged thickness was calculated by measuring the thickness of 50 different spots of the biofilm (n = 50).

Membranes	1st Run	4th Run	8th Run
Control	32.1 ± 18.8 μm	89.0 ± 12.9 μm	125.4 ± 41.4 μm
OMPs-feed	25.2 ± 10.2 μm	87.7 ± 21.9 μm	117.7 ± 29.4 μm

After FO experiments, we further carried out a SEM analysis on the pristine and fouled FO membrane surfaces, as shown in **Fig. S3**. It can be seen that the membrane surface was completely covered by foulants regardless of the presence of the OMPs. Interestingly, control seems to have a more fouled and rougher surface than OMPs-feed. To support this, the surface roughness of the FO membrane was analyzed using AFM. **Fig. S4** indicates that the pristine FO membrane showed a very smooth and clean surface (27.5 ± 3.1 nm) while the fouled surface of the FO membrane increased the average roughness (i.e., 100.7 ± 21.6 nm and 73.3 ± 29.1 nm, respectively). Besides, control exhibited higher surface roughness than OMPs-feed. An EDX analysis was then conducted to investigate the composition of the fouling layer. Results from **Table S1** show that the fouling layer of both control and OMPs-feed was mostly composed of high contents of carbon and oxygen elements (i.e., 71 ~ 72 % and 26 ~ 27 %, respectively), which supports the possible formation of the biofilm or organic fouling.

To further investigate the effect of biofouling on the surface functional groups, FT-IR analysis was conducted with the varying wavelength from 500 cm^{-1} to 4000 cm^{-1}. The results show that peaks of fouled FO membranes (Fig. 4) were different from those of the pristine FO membrane (**Fig. S5**), which indicates that the fouling layer completely covered the membrane surface. The assignments of the

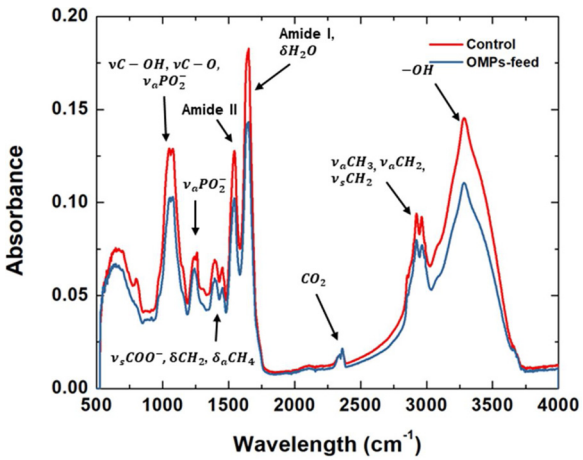

Fig. 4. FT-IR absorbance of the fouled membrane (control and OMPs) as a function of wavelength from 500 cm^{-1} to 4000 cm^{-1}. Detailed information on the assignments of FT-IR spectra of the fouled membrane surface is presented in **Table S2** (Kim et al., 2015b).

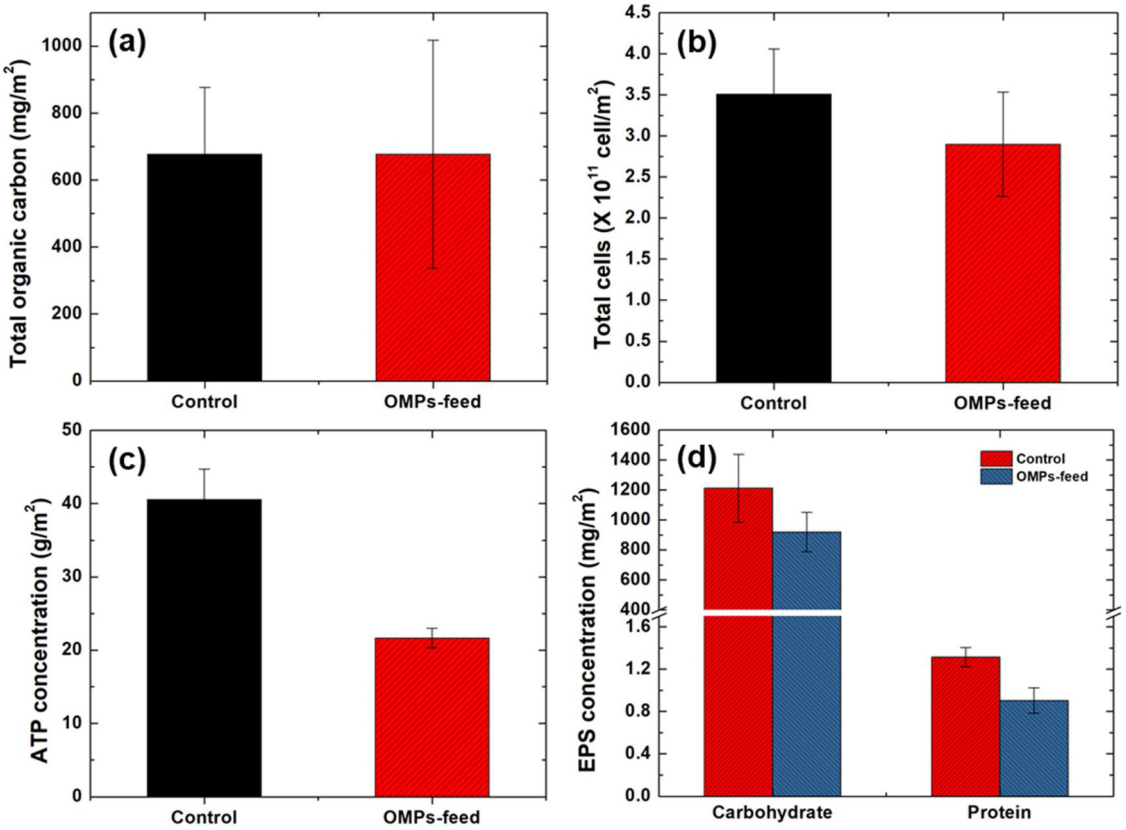

Fig. 5. Biofilm analysis of biofouled membranes with control and OMPs-feed: (a) DOC concentration, (b) total cell number, (c) ATP concentration, and (d) EPS concentration. The biofilm sample was collected from the membrane coupons after FO operation and then analyzed.

absorbance peaks in Fig. 4 were determined according to the literature (Kim et al., 2015b) and presented in **Table S4**. Fouled FO membrane exhibited peaks for several charged and apolar groups, and the overall absorbance of all peaks was reduced when spiking the OMPs in the FS compared to control. In particular, the peak absorbances of hydroxyl groups and stretching fatty chains (ν_aCH_3, ν_aCH_2, and ν_sCH_2) in cellular membranes were reduced by 23.9 % and 15.5 %, respectively. The absorbance of amide I and II peaks were also reduced by 21.6 % and 19.8 %, respectively. In addition, the peak absorbance of polysaccharides was reduced by 19.6 %. From these results, therefore, it may be implied that certain OMPs decelerate the growth of microorganisms because the peak intensity is related to the amount of the biofilm (Kim and Chong, 2017).

In order to evaluate the effect of the OMPs on the biofilm, the fouled membranes were collected and analyzed in terms of DOC, total cells, ATP concentration, and EPS concentration, as shown in Fig. 5. It is interesting to note that measured DOC values of control and OMPs-feed were similar (i.e., $677.2 \pm 199.7\,mg\,m^{-2}$ and $677.4 \pm 340.8\,mg\,m^{-2}$), which is consistent with measured thicknesses of the biofilm. On the other hand, total cell number on the fouled FO membrane of OMPs-feed ($2.9 \pm 0.6 \times 10^{11}$ cells m^{-2}) was slightly lower (approximately 15 %) compared to that of control ($3.5 \pm 0.5 \times 10^{11}$ cells m^{-2}). Besides, the ATP concentration of OMPs-feed ($21.7 \pm 1.3\,g\,m^{-2}$) was much smaller than that of control ($40.6 \pm 4.1\,g\,m^{-2}$). This could be because the OMPs used in this study consisted of antidepressants, beta-blockers, herbicides, stimulants, anticonvulsants, and antibiotics. In particular, both herbicides and antibiotics can inhibit the growth of bacteria (Kreisberg et al., 2013; Shockman and Lampen, 1962), which implies that the presence of OMPs such as herbicides and antibiotics could reduce the total cells and ATP concentrations in the biofilm layers.

To analyze the biofilm characteristics, EPS was extracted from the biofilm according to the procedure described in Section 2.4 and then analyzed in terms of carbohydrate and protein. Fig. 5**d** shows that control (i.e., $1{,}212 \pm 226\,mg\,m^{-2}$ and $1.3 \pm 0.1\,mg\,m^{-2}$, respectively) had higher concentrations of both carbohydrate and protein in EPS than OMPs-feed (i.e., $919 \pm 132\,mg\,m^{-2}$ and $0.9 \pm 0.1\,mg\,m^{-2}$, respectively). This indicates that the biofilm was more significantly formed on the membrane surface of control. In addition, EPS plays a significant role in determining the hydraulic resistance in membrane-based water treatment processes (Derlon et al., 2016). The ratio of EPS concentration to total cells was calculated to evaluate the impact of the OMPs on the production in EPS. Results showed the higher values of control for carbohydrate (i.e., 3.45×10^{-3} and 3.17×10^{-3} ng·cell^{-1}, respectively) and for protein, (i.e., 3.75×10^{-6} and 3.12×10^{-6} ng·cell^{-1}, respectively) compared to OMPs-feed. This implies that the presence of certain OMPs may be able to inhibit not only the biofilm growth but also the EPS production. Consequently, these results can conclude that even though the biofilm has a similar thickness, the composition of the biofilm can lead to different behavior in water flux probably due to the nature and characteristics of the biofilm (Kerdi et al., 2019).

Fig. 6 presents the FEEM plots of EPS samples extracted from the fouled FO membranes and divided into three regions. Region I, II, and III indicate protein-like matters (E_x = 250 nm–280 nm and E_m < 380 nm), tyrosine-like proteins (E_x = 220 nm–250 nm and E_m = 330 nm–380 nm), and humic-like matters (E_x > 280 nm and E_m > 380 nm), respectively (Kim et al., 2015b). Relative intensities of all regions are summarized in **Table S3**. When comparing OMPs-feed to control, FEEM intensities were reduced by 15.3 %, 10.1 %, and 19.4 % for protein-like matters, tyrosine-like proteins, and humic-like matters, respectively. The FEEM plots support the result of reduced EPS concentration under the presence of OMPs compared to control (Fig. 5d). This implies that OMPs could inhibit the production of EPS in the biofilm layer.

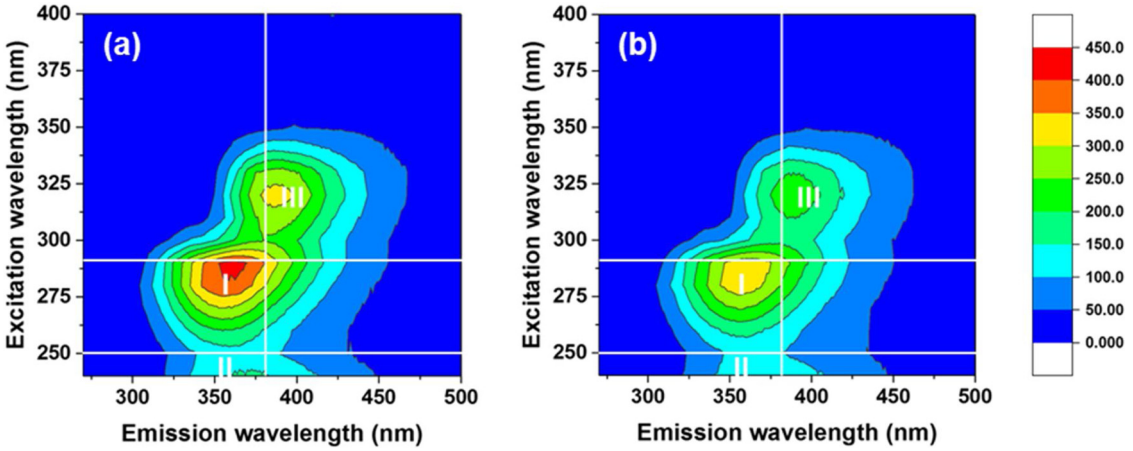

Fig. 6. FEEM plots of EPS extracted from the fouled membrane surface: (a) control, and (b) OMPs-feed. Regions I, II, and III indicate protein-like matters, tyrosine-like proteins, and humic-like matters, respectively. FEEM analyses have been shown of importance to evaluate fouling (Sanawar et al., 2018).

3.3. Impact of organic micropollutants (OMPs) on bacterial community composition in biofilm layers

In order to investigate the effect of the OMPs on the biofilm in detail, we analyzed the bacterial community composition via a NGS analysis on the primary wastewater and the biofilm samples. The biofilm samples were collected from the fouled FO membranes after FO experiments (see Fig. 7). In the primary wastewater, *Cloacibacterium* (14.9 %) was the most dominant species followed by *Comamonas* (7.8 %), *Arcobacter* (7.2 %), *Acidovorax* (4.1 %), *Veillonella* (3.4 %), and *Azonexus* (2.8 %). *Cloacibacterium* species are often found in municipal wastewater (Allen et al., 2006). *Comamonas* and *Acidovorax* are denitrifying bacteria that converts nitrate nitrogen to nitrogen gas (Gumaelius et al., 2001; Heylen et al., 2008), and *Veillonella* is a lactate fermenting anaerobic bacterium (Rogosa, 1964). This indicates that the transport of wastewater from houses to a wastewater treatment plant occurred under the anoxic condition. *Arcobacter* species are known as one of the pathogenic bacteria (Miller et al., 2007).

Fig. 7 shows that *Aquicella* (19.0 %) was most dominant followed by *Pseudarcicella* (17.4 %), *Mitsuaria* (12.3 %), *Cupriavidus* (6.2 %), *Methylophilus* (5.2 %), *Bradyrhizobium* (5.1 %), *Bosea* (2.84 %), *Legionella* (2.4 %), etc. in the biofilm of control. All major bacteria require the aerobic condition for the growth (Santos et al., 2003; Kampfer et al., 2012; Amakata et al., 2005; Nurhayati et al., 2014; Jenkins et al., 1987; Zhang et al., 2012; Ouattara et al., 2003) due to the condition of FO operation (i.e., the open system). It should be noted that *Legionella* (i.e., a pathogenic group causing Legionnaires' disease and Pontiac fever (Fields et al., 2002)) was observed, which implies the potential problem in the system. However, the multiple-barrier effect by both FO and RO membranes, as well as their non-porous structure can highly reject

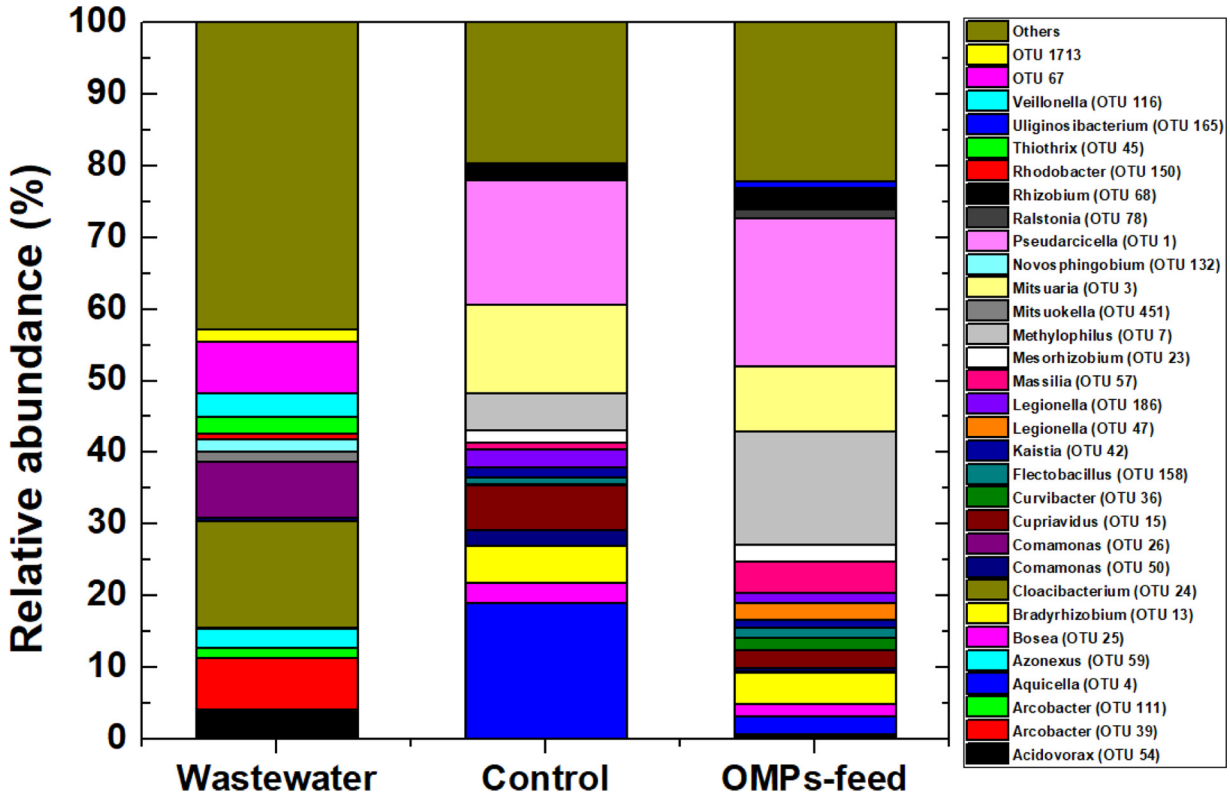

Fig. 7. Variations of bacterial community composition of primary wastewater and biofilm (i.e., control and OMPs-feed).

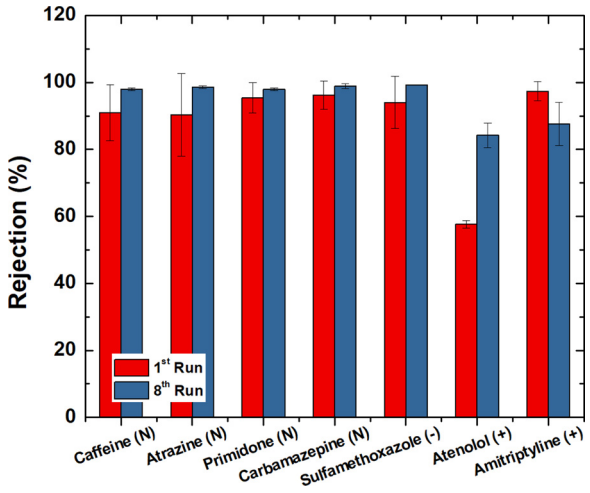

Fig. 8. Rejections of seven OMP compounds at 1st run and 8th run of the FO operation. The order of the OMPs is determined based on their molecular weight. (N), (-), and (+) indicate neutral, negative, and positive charges, respectively.

harmful bacteria, which can secure the safety of the product water (Kim et al., 2019b).

The results from Fig. 7 also show that the bacterial community composition of the biofilm was dynamically changed from that of primary wastewater. The dominant species of primary wastewater became the minor species as *Comamonas* and *Acidovorax* reduced from 7.8 % and 4.1 %–2.2 % and 0.1 %, respectively, and other species (i.e., *Cloacibacterium*, *Arcobacter*, *Veillonella*, and *Azonexus*) became negligible. There are four possible reasons for this significant difference in the bacterial community composition between primary wastewater and the biofilm on the membrane surface. The first can be the different attachment properties of bacteria. Bacteria suspended in a solution approach to the membrane surface and experience the hydrodynamic and physicochemical forces (Bos et al., 1999). Therefore, the bacterial attachment can be determined from their motility, density, surface charges, and surface hydrophobicity (Tuson and Weibel, 2013). A second explanation could be a difference in the condition (e.g., aerobic, anaerobic, and anoxic conditions). Primary wastewater might experience an anoxic or anaerobic condition during the transport of wastewater through the sewer from the houses to the wastewater treatment plant (Jelic et al., 2015), which can be supported by some anoxic and anaerobic bacteria, as shown in Fig. 7. However, our lab-scale FO experimental unit was operated under the open system, which assumes the slightly aerobic condition. The third reason can be the effect of reverse salt flux (RSF). During the FO operation, highly concentrated DS was diffused to the feed side (Lee et al., 2010), and hence bacteria attached on the membrane surface could suffer from an elevated salinity concentration affecting the inoculated microbial community composition, resulting in a lower diversity (Li et al., 2017a). In other words, the growth of more salt-tolerant bacteria could be selected on the membrane (Rath et al., 2019). The last reason might be due to the injection of methanol to the FS. For a fair comparison with OMPs-feed, 20 μL of methanol was spiked to the 2 L of FS. This could influence the bacterial community composition of the biofilm because methanol can be an additional carbon source (Sun et al., 2016). Nevertheless, this effect would be restricted due to its much lower concentration (0.25 mM) compared to that (40 mM) of other studies (Vishnivetskaya et al., 2010).

We further compared the bacterial community composition of the biofilm between control and OMPs-feed. In the biofilm of OMPs-feed, the most dominant species was *Pseudarcicella* (20.7 %) followed by *Methylophilus* (15.9 %), *Mitsuaria* (9.0 %), *Massilia* (4.5 %), *Bradyrhizobium* (4.4 %), *Rhizobium* (3.0 %), *Aquicella* (2.5 %), *Cupriavidus* (2.5 %), *Legionella* (2.4 %), etc. as shown in Fig. 7. From these results, it can be seen that OMPs-feed exhibited similar composition but different percentages compared to control. For example, when comparing OMPs-feed to control, *Aquicella* was reduced from 19.0 %–2.5 %, and *Methylophilus* was increased from 5.2%–15.9%. Therefore, it can be said that the OMPs used in this study could inhibit the growth of some specific bacteria on the membrane surface.

In addition to the bacterial community composition, the bacterial diversity was also investigated in terms of the Shannon index (i.e., the measure of species diversity in a given community). A high value represents a diverse and equally distributed community, while a lower value indicates a less diverse community (Morris et al., 2014). Shannon indexes calculated based on the pyrosequencing data were 4.2 ± 0.1, 3.3 ± 0.2, and 2.8 ± 0.3 for primary wastewater, control, and OMPs-feed, respectively. This indicates that primary wastewater had the most diverse bacterial community, followed by control and OMPs-feed. As discussed above, microorganisms were selectively attached and grew on the membrane surface, and therefore the bacterial diversity was reduced during FO operation. Furthermore, the bacterial diversity was more decreased when the OMPs were spiked in the FS. This was because the OMPs used in this study contained herbicides and antibiotics and thus induced the harmful impact on the microorganisms. In conclusion, the OMPs in the FS influenced the bacterial community composition and decreased bacterial diversity.

3.4. Impact of biofouling on the rejection of organic micropollutants (OMPs) in FO

The effect of the biofilm on the transport of the OMPs was investigated by measuring the rejection rates of the OMPs after the 1st run and 8th run of FO operation. Fig. 8 shows that six OMPs (amitriptyline hydrochloride, atrazine, caffeine, carbamazepine, primidone, sulfamethoxazole) exhibited higher OMPs rejection rates than 90 % except for atenolol. Besides, it is observed that the rejection rate of the OMPs having neutral charges generally increased when increasing their molecular weights. This is because steric hindrance is a dominant mechanism of the OMPs transport through the FO membrane (Kim et al., 2017a; Kim et al., 2019a), which means that the OMPs having higher molecular weight are more readily rejected by the FO membrane. In the case of the OMPs having positive charges, different behaviors of the OMPs rejection rates were observed. Atenolol showed the lowest OMPs rejection rate despite its higher molecular weight than the OMPs having neutral charges, while amitriptyline hydrochloride exhibited the highest OMPs rejection rate. Due to the positive charge, atenolol can be easily absorbed on the negatively charged FO membrane, which induced higher electrostatic attraction and hence resulted in higher transport of atenolol to the DS (Kim et al., 2019a). Amitriptyline hydrochloride (313.9 g mol^{-1}) has a much higher molecular weight compared to other OMPs (215.7 ~ 266.3 g mol^{-1}), as shown in Table 2. Therefore, steric hindrance became a dominant mechanism rather than an electrostatic attraction for amitriptyline hydrochloride, thereby causing the highest rejection rate.

In 8th run (i.e., the biofilm was developed, as shown in Fig. 3), rejection rates of the OMPs having neutral charges were significantly enhanced to 98 ~ 99 %. There are two potential reasons: (i) biodegradation of the OMPs and (ii) an increase in mass transfer resistance by the biofilm. The biofilm is a mixture of microorganisms that biodegrade organics, and therefore the OMPs can be degraded through the biofilm because the OMPs are organic matters (Petropavlovskii and Sillanpää, 2013). Besides, the biofilm can play and act like an additional resistant layer and hence increase the hydraulic resistance of the FO membrane to the OMPs (Herzberg and Elimelech, 2007). Interestingly, OMPs having positive charges exhibited different behaviors, and the rejection rate of atenolol was greatly enhanced while that of amitriptyline hydrochloride decreased. As discussed above, the biofilm increased the hydraulic resistance to the OMPs, thereby led to an increase in the

rejection rate of atenolol from 57.6%–84.2%. However, this value was still lower than the rejection rates of other OMPs. Similar to the FO membrane surface, the biofilm also has a negatively charged surface (Dertli et al., 2015; Li et al., 2017b), and therefore, the OMPs having positive charges could be readily adsorbed on the biofilm. Consequently, atenolol could be readily transported to the DS, and the effect of the biofilm on the rejection rate was limited. On the contrary to atenolol, amitriptyline hydrochloride exhibited decreased rejection rate from 97.4%–87.7% after membrane fouling occurred. It can be hypothesized that amitriptyline hydrochloride was more accumulated in the biofilm due to the electrostatic attraction, and hence the actual concentration would be much higher than the amount we spiked to the fresh FS every day. Therefore, the rejection rate of amitriptyline hydrochloride became reduced and lower than those of other OMPs despite its highest molecular weight among the OMPs. However, further study is required to prove this hypothesis.

The findings from this study have a significant implication for optimizing osmotic dilution in FO operation and OMPs rejection. An increase in OMPs rejection by the biofilm may enable to increase OMPs concentrations on the active layer, potentially leading to the increased OMPs concentration in the biofilm layers. Then, a certain OMPs will function as biofilm control agents. Nevertheless, the fate and extent of biodegradability of OMPs may need additional research by using actual seawater as DS and additional tests to incubate OMPs with a microbial community mixture will be required.

4. Conclusions

In the present study, we systematically investigated FO membranes for seawater desalination and wastewater reclamation with a particular focus on biofouling when municipal wastewater contains OMPs. FO membrane performance was investigated with (OMPs-feed) and without (control) OMPs in the feed solution. The seven different OMPs were amitriptyline hydrochloride, atenolol, atrazine, caffeine, carbamazepine, primidone, and sulfamethoxazole. At the same time, biofilm growth was monitored using OCT. The accumulated biofilm on the membrane surface and its bacterial community composition were analyzed using e.g. FEEM. Lastly, the transport behavior of the OMPs was evaluated in terms of rejection rates. The main findings drawn from the present study can be summarized briefly as follows:

- Biofouling on the FO membrane feed side showed (i) a lower flux decline in the presence of OMPs in the feed water and (ii) a higher OMPs rejection, both illustrating better membrane performance.
- OMPs did not affect the biofilm spatial structure and thickness and DOC concentration. On the other hand, OMPs influenced the biofilm composition resulting in a lower concentrations of cells, ATP, and EPS compared to the control without OMPs.
- The bacterial community composition of the biofouling layer at the feed side (wastewater) of the FO membrane was significantly different from that of municipal wastewater. OMPs could affect the bacterial community composition and the bacterial diversity in the biofilm compared to the control.

CRediT authorship contribution statement

Youngjin Kim: Conceptualization, Data curation, Formal analysis, Investigation, Methodology, Writing - original draft, Writing - review & editing. **Lan Hee Kim:** Conceptualization, Data curation, Formal analysis, Investigation, Methodology, Writing - original draft, Writing - review & editing. **Johannes S. Vrouwenvelder:** Conceptualization, Formal analysis, Investigation, Methodology, Writing - review & editing. **Noreddine Ghaffour:** Conceptualization, Formal analysis, Investigation, Methodology, Writing - review & editing.

Declaration of Competing Interest

The authors declare that they have no known competing financial interests or personal relationships that could have appeared to influence the work reported in this paper.

Acknowledgements

The research reported in this paper was supported by King Abdullah University of Science and Technology (KAUST), Saudi Arabia, through Competitive Research Grant Program - CRG2017 (CRG6), Project # UFR/1/3404-01. Authors extend their gratitude to the Water Desalination and Reuse Center (WDRC) staff for their continuous support.

Appendix A. Supplementary data

Supplementary material related to this article can be found, in the online version, at doi:https://doi.org/10.1016/j.jhazmat.2020.123386.

References

Akther, N., Phuntsho, S., Chen, Y., Ghaffour, N., Shon, H.K., 2019. Recent advances in nanomaterial-modified polyamide thin-film composite membranes for forward osmosis processes. J. Membr. Sci. 584, 20–45.
Albertsen, M., Karst, S.M., Ziegler, A.S., Kirkegaard, R.H., Nielsen, P.H., 2015. Back to basics – the influence of DNA extraction and primer choice on phylogenetic analysis of activated sludge communities. PLoS One 10, e0132783.
Allen, T.D., Lawson, P.A., Collins, M.D., Falsen, E., Tanner, R.S., 2006. Cloacibacterium normanense gen. nov., sp. nov., a novel bacterium in the family Flavobacteriaceae isolated from municipal wastewater. Int. J. Syst. Evol. Microbiol. 56, 1311–1316.
Amakata, D., Matsuo, Y., Shimono, K., Park, J.K., Yun, C.S., Matsuda, H., Yokota, A., Kawamukai, M., 2005. Mitsuaria chitosanitabida gen. nov., sp. nov., an aerobic, chitosanase-producing member of the 'Betaproteobacteria'. Int. J. Syst. Evol. Microbiol. 55, 1927–1932.
Attarde, D., Jain, M., Singh, P.K., Gupta, S.K., 2017. Energy-efficient seawater desalination and wastewater treatment using osmotically driven membrane processes. Desalination 413, 86–100.
Badran, A., 2017. Climate change and water science policy in management. In: Murad, S., Baydoun, E., Daghir, N. (Eds.), Water, Energy & Food Sustainability in the Middle East: The Sustainability Triangle. Springer International Publishing, Cham, pp. 3–19.
Bamaga, O.A., Yokochi, A., Zabara, B., Babaqi, A.S., 2011. Hybrid FO/RO desalination system: preliminary assessment of osmotic energy recovery and designs of new FO membrane module configurations. Desalination 268, 163–169.
Barragán, J.M., de Andrés, M., 2015. Analysis and trends of the world's coastal cities and agglomerations. Ocean Coast. Manage. 114, 11–20.
Blandin, G., Verliefde, A.R.D., Tang, C.Y., Le-Clech, P., 2015. Opportunities to reach economic sustainability in forward osmosis–reverse osmosis hybrids for seawater desalination. Desalination 363, 26–36.
Boo, C., Elimelech, M., Hong, S., 2013. Fouling control in a forward osmosis process integrating seawater desalination and wastewater reclamation. J. Membr. Sci. 444, 148–156.
Bos, R., van der Mei, H.C., Busscher, H.J., 1999. Physico-chemistry of initial microbial adhesive interactions–its mechanisms and methods for study. FEMS Microbiol. Rev. 23, 179–230.
Bucs, S.S., Valladares Linares, R., Vrouwenvelder, J.S., Picioreanu, C., 2016. Biofouling in forward osmosis systems: an experimental and numerical study. Water Res. 106, 86–97.
Caporaso, J.G., Lauber, C.L., Walters, W.A., Berg-Lyons, D., Huntley, J., Fierer, N., Owens, S.M., Betley, J., Fraser, L., Bauer, M., Gormley, N., Gilbert, J.A., Smith, G., Knight, R., 2012. Ultra-high-throughput microbial community analysis on the Illumina HiSeq and MiSeq platforms. ISME J. 6, 1621.
Cath, T.Y., Hancock, N.T., Lundin, C.D., Hoppe-Jones, C., Drewes, J.E., 2010. A multi-barrier osmotic dilution process for simultaneous desalination and purification of impaired water. J. Membr. Sci. 362, 417–426.
Choi, B.G., Kim, D.I., Hong, S., 2016. Fouling evaluation and mechanisms in a FO-RO hybrid process for direct potable reuse. J. Membr. Sci. 520, 89–98.
Choi, B.G., Zhan, M., Shin, K., Lee, S., Hong, S., 2017. Pilot-scale evaluation of FO-RO osmotic dilution process for treating wastewater from coal-fired power plant integrated with seawater desalination. J. Membr. Sci. 540, 78–87.
Derlon, N., Grütter, A., Brandenberger, F., Sutter, A., Kuhlicke, U., Neu, T.R., Morgenroth, E., 2016. The composition and compression of biofilms developed on ultrafiltration membranes determine hydraulic biofilm resistance. Water Res. 102, 63–72.
Dertli, E., Mayer, M.J., Narbad, A., 2015. Impact of the exopolysaccharide layer on biofilms, adhesion and resistance to stress in Lactobacillus johnsonii FI9785. BMC Microbiol. 15 8-8.
Dreszer, C., Wexler, A.D., Drusová, S., Overdijk, T., Zwijnenburg, A., Flemming, H.C., Kruithof, J.C., Vrouwenvelder, J.S., 2014. In-situ biofilm characterization in membrane systems using optical coherence tomography: formation, structure, detachment

and impact of flux change. Water Res. 67, 243–254.
Edgar, R.C., 2013. UPARSE: highly accurate OTU sequences from microbial amplicon reads. Nat. Methods 10, 996.
Fields, B.S., Benson, R.F., Besser, R.E., 2002. Legionella and Legionnaires' disease: 25 years of investigation. Clin. Microbiol. Rev. 15, 506–526.
Fortunato, L., Jang, Y., Lee, J.-G., Jeong, S., Lee, S., Leiknes, T., Ghaffour, N., 2018. Fouling development in direct contact membrane distillation: non-invasive monitoring and destructive analysis. Water Res. 132, 34–41.
Ghaffour, N., Missimer, T.M., Amy, G.L., 2013. Technical review and evaluation of the economics of water desalination: current and future challenges for better water supply sustainability. Desalination 309, 197–207.
Giwa, A., Dindi, A., Kujawa, J., 2019. Membrane bioreactors and electrochemical processes for treatment of wastewaters containing heavy metal ions, organics, micropollutants and dyes: recent developments. J. Hazard. Mater. 370, 172–195.
Gumaelius, L., Magnusson, G., Pettersson, B., Dalhammar, G., 2001. Comamonas denitrificans sp. nov., an efficient denitrifying bacterium isolated from activated sludge. Int. J. Syst. Evol. Microbiol. 51, 999–1006.
Hancock, N.T., Black, N.D., Cath, T.Y., 2012. A comparative life cycle assessment of hybrid osmotic dilution desalination and established seawater desalination and wastewater reclamation processes. Water Res. 46, 1145–1154.
Hancock, N.T., Xu, P., Roby, M.J., Gomez, J.D., Cath, T.Y., 2013. Towards direct potable reuse with forward osmosis: technical assessment of long-term process performance at the pilot scale. J. Membr. Sci. 445, 34–46.
Herzberg, M., Elimelech, M., 2007. Biofouling of reverse osmosis membranes: role of biofilm-enhanced osmotic pressure. J. Membr. Sci. 295, 11–20.
Heylen, K., Lebbe, L., De Vos, P., 2008. Acidovorax caeni sp. nov., a denitrifying species with genetically diverse isolates from activated sludge. Int. J. Syst. Evol. Microbiol. 58, 73–77.
Jelic, A., Rodriguez-Mozaz, S., Barceló, D., Gutierrez, O., 2015. Impact of in-sewer transformation on 43 pharmaceuticals in a pressurized sewer under anaerobic conditions. Water Res. 68, 98–108.
Jenkins, O., Byrom, D., Jones, D., 1987. Methylophilus: a new genus of methanol-utilizing bacteria. Int. J. Syst. Evol. Microbiol. 37, 446–448.
Jin, X., Shan, J., Wang, C., Wei, J., Tang, C.Y., 2012. Rejection of pharmaceuticals by forward osmosis membranes. J. Hazard. Mater. 227-228, 55–61.
Kampfer, P., Busse, H.J., Longaric, I., Rossello-Mora, R., Galatis, H., Lodders, N., 2012. Pseudarcicella hirudinis gen. nov., sp. nov., isolated from the skin of the medical leech Hirudo medicinalis. Int. J. Syst. Evol. Microbiol. 62, 2247–2251.
Kerdi, S., Qamar, A., Alpatova, A., Ghaffour, N., 2019. An in-situ technique for the direct structural characterization of biofouling in membrane filtration. J. Membr. Sci. 583, 81–92.
Kim, L.H., Chong, T.H., 2017. Physiological responses of salinity-stressed vibrio sp. and the effect on the biofilm formation on a nanofiltration membrane. Environ. Sci. Technol. 51, 1249–1258.
Kim, J.E., Phuntsho, S., Ali, S.M., Choi, J.Y., Shon, H.K., 2018. Forward osmosis membrane modular configurations for osmotic dilution of seawater by forward osmosis and reverse osmosis hybrid system. Water Res. 128, 183–192.
Kim, Y., Li, S., Ghaffour, N., 2020. Evaluation of different cleaning strategies for different types of forward osmosis membrane fouling and scaling. J. Membr. Sci. 596, 117731.
Kim, Y., Li, S., Chekli, L., Woo, Y.C., Wei, C.-H., Phuntsho, S., Ghaffour, N., Leiknes, T., Shon, H.K., 2017a. Assessing the removal of organic micro-pollutants from anaerobic membrane bioreactor effluent by fertilizer-drawn forward osmosis. J. Membr. Sci. 533, 84–95.
Kim, D.I., Kim, J., Shon, H.K., Hong, S., 2015a. Pressure retarded osmosis (PRO) for integrating seawater desalination and wastewater reclamation: energy consumption and fouling. J. Membr. Sci. 483, 34–41.
Kim, Y., Li, S., Phuntsho, S., Xie, M., Shon, H.K., Ghaffour, N., 2019a. Understanding the organic micropollutants transport mechanisms in the fertilizer-drawn forward osmosis process. J. Environ. Manage. 248, 109240.
Kim, Y., Woo, Y.C., Phuntsho, S., Nghiem, L.D., Shon, H.K., Hong, S., 2017b. Evaluation of fertilizer-drawn forward osmosis for coal seam gas reverse osmosis brine treatment and sustainable agricultural reuse. J. Membr. Sci. 537, 22–31.
Kim, L.H., Jung, Y., Yu, H.-W., Chae, K.-J., Kim, I.S., 2015b. Physicochemical interactions between rhamnolipids and pseudomonas aeruginosa biofilm layers. Environ. Sci. Technol. 49, 3718–3726.
Kim, Y., Li, S., Francis, L., Li, Z., Linares, R.V., Alsaadi, A.S., Abu-Ghdaib, M., Son, H.S., Amy, G., Ghaffour, N., 2019b. Osmotically and thermally isolated forward osmosis–membrane distillation (FO–MD) integrated module. Environ. Sci. Technol. 53, 3488–3498.
Kook, S., Lee, C., Nguyen, T.T., Lee, J., Shon, H.K., Kim, I.S., 2018. Serially connected forward osmosis membrane elements of pressure-assisted forward osmosis-reverse osmosis hybrid system: process performance and economic analysis. Desalination 448, 1–12.
Kreisberg, J.F., Ong, N.T., Krishna, A., Joseph, T.L., Wang, J., Ong, C., Ooi, H.A., Sung, J.C., Siew, C.C., Chang, G.C., Biot, F., Cuccui, J., Wren, B.W., Chan, J., Sivalingam, S.P., Zhang, L.-H., Verma, C., Tan, P., 2013. Growth inhibition of pathogenic bacteria by sulfonylurea herbicides. Antimicrob. Agents Chemother. 57, 1513–1517.
Lee, J., Ghaffour, N., 2019. Predicting the performance of large-scale forward osmosis module using spatial variation model: effect of operating parameters including temperature. Desalination 469, 114095.
Lee, S., Boo, C., Elimelech, M., Hong, S., 2010. Comparison of fouling behavior in forward osmosis (FO) and reverse osmosis (RO). J. Membr. Sci. 365, 34–39.
Li, S., Kim, Y., Chekli, L., Phuntsho, S., Shon, H.K., Leiknes, T., Ghaffour, N., 2017a. Impact of reverse nutrient diffusion on membrane biofouling in fertilizer-drawn forward osmosis. J. Membr. Sci. 539, 108–115.
Li, S., Kim, Y., Chekli, L., Phuntsho, S., Shon, H.K., Leiknes, T., Ghaffour, N., 2017b. Impact of reverse nutrient diffusion on membrane biofouling in fertilizer-drawn forward osmosis. J. Membr. Sci. 539, 108–115.
Liu, J., Wen, J., Huang, Y., Shi, M., Meng, Q., Ding, J., Xu, H., 2015. Human settlement and regional development in the context of climate change: a spatial analysis of low elevation coastal zones in China. Mitig. Adapt. Strat. Glob. Change 20, 527–546.
Magoč, T., Salzberg, S.L., 2011. FLASH: fast length adjustment of short reads to improve genome assemblies. Bioinformatics (Oxford, England) 27, 2957–2963.
Miller, W.G., Parker, C.T., Rubenfield, M., Mendz, G.L., Wösten, M.M.S.M., Ussery, D.W., Stolz, J.F., Binnewies, T.T., Hallin, P.F., Wang, G., Malek, J.A., Rogosin, A., Stanker, L.H., Mandrell, R.E., 2007. The complete genome sequence and analysis of the Epsilonproteobacterium Arcobacter butzleri. PLOS One 2, e1358.
Morris, E.K., Caruso, T., Buscot, F., Fischer, M., Hancock, C., Maier, T.S., Meiners, T., Müller, C., Obermaier, E., Prati, D., Socher, S.A., Sonnemann, I., Wäschke, N., Wubet, T., Wurst, S., Rillig, M.C., 2014. Choosing and using diversity indices: insights for ecological applications from the German Biodiversity Exploratories. Ecol. Evol. 4, 3514–3524.
Nurhayati, R.W., Ojima, Y., Kitatsuji, S., Suryadarma, P., Taya, M.J.Ao.M., 2014. An aerobic formate-utilizing bacterium, Cupriavidus sp., isolated from activated sludge of wastewater treatment. An. Microbiol. 64, 869–873.
Ouattara, A.S., Assih, E.A., Thierry, S., Cayol, J.L., Labat, M., Monroy, O., Macarie, H., 2003. Bosea minatitlanensis sp. nov., a strictly aerobic bacterium isolated from an anaerobic digester. Int. J. Syst. Evol. Microbiol. 53, 1247–1251.
Petropavlovskii, A., Sillanpää, M., 2013. Removal of micropollutants by biofilms: current approaches and future prospects. Environ. Technol. Rev. 2, 29–44.
Rath, K.M., Fierer, N., Murphy, D.V., Rousk, J., 2019. Linking bacterial community composition to soil salinity along environmental gradients. ISME J. 13, 836–846.
Rogosa, M., 1964. The genus Veillonella. I. General cultural, ecological, and biochemical considerations. J. Bacteriol. 87, 162–170.
Sanawar, H., Pinel, I., Farhat, N.M., Bucs, S.S., Zlopasa, J., Kruithof, J.C., Witkamp, G.J., van Loosdrecht, M.C.M., Vrouwenvelder, J.S., 2018. Enhanced biofilm solubilization by urea in reverse osmosis membrane systems. Water Res. X (1), 100004.
Santos, P., Pinhal, I., Rainey, F.A., Empadinhas, N., Costa, J., Fields, B., Benson, R., Verissimo, A., Da Costa, M.S., 2003. Gamma-proteobacteria Aquicella lusitana gen. nov., sp. nov., and Aquicella siphonis sp. nov. infect protozoa and require activated charcoal for growth in laboratory media. Appl. Environ. Microbiol. 69, 6533–6540.
Shockman, G.D., Lampen, J.O., 1962. Inhibition by antibiotics of the growth of bacterial and yeast protoplasts. J. Bacteriol. 84, 508–512.
Smith, K., Liu, S., 2017. Energy for conventional water supply and wastewater treatment in Urban China: a review. Glob. Challenges 1, 1600016.
Sun, Y., Shen, D., Zhou, X., Shi, N., Tian, Y., 2016. Microbial diversity and community structure of denitrifying biological filters operated with different carbon sources. Springerplus 5 1752-1752.
Tuson, H.H., Weibel, D.B., 2013. Bacteria-surface interactions. Soft Matter 9, 4368–4380.
Valladares Linares, R., Yangali-Quintanilla, V., Li, Z., Amy, G., 2011. Rejection of micropollutants by clean and fouled forward osmosis membrane. Water Res. 45, 6737–6744.
Valladares Linares, R., Li, Z., Yangali-Quintanilla, V., Ghaffour, N., Amy, G., Leiknes, T., Vrouwenvelder, J.S., 2016a. Life cycle cost of a hybrid forward osmosis – low pressure reverse osmosis system for seawater desalination and wastewater recovery. Water Res. 88, 225–234.
Valladares Linares, R., Wexler, A.D., Bucs, S.S., Dreszer, C., Zwijnenburg, A., Flemming, H.C., Kruithof, J.C., Vrouwenvelder, J.S., 2016b. Compaction and relaxation of biofilms. Desalin. Water Treat. 57, 12902–12914.
Vishnivetskaya, T.A., Brandt, C.C., Madden, A.S., Drake, M.M., Kostka, J.E., Akob, D.M., Küsel, K., Palumbo, A.V., 2010. Microbial community changes in response to ethanol or methanol amendments for U(VI) reduction. Appl. Environ. Microbiol. 76, 5728.
Volpin, F., Fons, E., Chekli, L., Kim, J.E., Jang, A., Shon, H.K., 2018. Hybrid forward osmosis-reverse osmosis for wastewater reuse and seawater desalination: understanding the optimal feed solution to minimise fouling. Process Saf. Environ. Protect. 117, 523–532.
Volpin, F., Yu, H., Cho, J., Lee, C., Phuntsho, S., Ghaffour, N., Vrouwenvelder, J.S., Shon, H.K., 2019. Human urine as a forward osmosis draw solution for the application of microalgae dewatering. J. Hazard. Mater. 378, 120724.
Wang, Q., Garrity, G.M., Tiedje, J.M., Cole, J.R., 2007. Naïve Bayesian classifier for Rapid assignment of rRNA sequences into the new bacterial taxonomy. Appl. Environ. Microbiol. 73, 5261–5267.
Wei, X., Binger, Z.M., Achilli, A., Sanders, K.T., Childress, A.E., 2019. A modeling framework to evaluate blending of seawater and treated wastewater streams for synergistic desalination and potable reuse. Water Res., 115282.
Wei, C.-H., Hoppe-Jones, C., Amy, G., Leiknes, T., 2015. Organic micro-pollutants' removal via anaerobic membrane bioreactor with ultrafiltration and nanofiltration. J. Water Reuse Desalin. 6, 362–370.
Xie, M., Gray, S.R., 2016. Transport and accumulation of organic matter in forward osmosis-reverse osmosis hybrid system: mechanism and implications. Sep. Purif. Technol. 167, 6–16.
Xie, M., Price, W.E., Nghiem, L.D., Elimelech, M., 2013. Effects of feed and draw solution temperature and transmembrane temperature difference on the rejection of trace organic contaminants by forward osmosis. J. Membr. Sci. 438, 57–64.
Xie, M., Nghiem, L.D., Price, W.E., Elimelech, M., 2012a. Comparison of the removal of hydrophobic trace organic contaminants by forward osmosis and reverse osmosis. Water Res. 46, 2683–2692.
Xie, M., Nghiem, L.D., Price, W.E., Elimelech, M., 2014a. Relating rejection of trace organic contaminants to membrane properties in forward osmosis: measurements, modelling and implications. Water Res. 49, 265–274.
Xie, M., Price, W.E., Nghiem, L.D., 2012b. Rejection of pharmaceutically active compounds by forward osmosis: role of solution pH and membrane orientation. Sep.

Purif. Technol. 93, 107–114.
Xie, M., Nghiem, L.D., Price, W.E., Elimelech, M., 2014b. Impact of organic and colloidal fouling on trace organic contaminant rejection by forward osmosis: role of initial permeate flux. Desalination 336, 146–152.
Zhang, Y.M., Li, Y., Chen, W.F., Wang, E.T., Sui, X.H., Li, Q.Q., Zhang, Y.Z., Zhou, Y.G., Chen, W.X., 2012. Bradyrhizobium huanghuaihaiense sp. nov., an effective symbiotic bacterium isolated from soybean (Glycine max L.) nodules. Int. J. Syst. Evol. Microbiol. 62, 1951–1957.
Żur, J., Piński, A., Marchlewicz, A., Hupert-Kocurek, K., Wojcieszyńska, D., Guzik, U., 2018. Organic micropollutants paracetamol and ibuprofen-toxicity, biodegradation, and genetic background of their utilization by bacteria. Environ. Sci. Pollut. Res. Int. 25, 21498–21524.